

Figure S1. Ray paths and examples of data analysis. (A) Geometry of ray paths from a deep Philippines earthquake (20100724, depth = 555 km) to the USArray. Geometrical ray paths of SKS (black) and SKKS (cyan) assuming the reference model PREM at epicentral distances of 110° to 125° are displayed along with a less conventional path, SP_dKS and SKP_dS (red). Note the similarity in mantle paths with this phase and SKS at ranges less than 115° . (B) Surface projection of the ray paths at two different azimuthal ranges. The USArray stations are marked as black triangles with over 400 stations available. The sampling region at CMB of SP_dKS and SKP_dS are indicated as blue and green patches. Note that the sampling area in our study is away from the Central Pacific LLSVP. (C) The sampling region of SP_dKS (left) and SKP_dS (right) at the CMB for three events used in this study.

Figure S2. The comparison between data records (black) and MPD simulations (red) for $SKS+SKS_d$ phases at different distance ranges. Shaded zones indicate anomalous waveforms, which suggest strong lateral variations. The data in the MPD process are filtered with a bandpass filter (5-50 sec).

Figure S3. Examples of the height inversion process. The synthetics (black) library is generated with GRT method for one-side low velocity layer model with different thickness H . In the layer: (A) $\delta V_s = -6\%$, $\delta V_p = -2\%$; (B) $\delta V_s = -8\%$, $\delta V_p = -5\%$. The red traces are the stacked records within azimuth $29^\circ-37^\circ$ as in Figure 2C. For a particular distance, we cross-correlated the data with the synthetics across the library to find the H value with the best cross-correlation coefficient. On the top left, combined height-distance profiles are displayed.

Figure S4. Inverted elevation map of the Low Velocity Zone above the CMB for the three events. The elevation map was migrated to CMB on both source side (top row) and receiver side (bottom row). To accommodate the Fresnel zone, we apply smoothing on the original inverted results with 2.5 deg radius to get the combined map (right column).

Figure S5. Validation of SKS synthetics generated with the FD against those from (A) $f-k$ and (B) GRT method. FD agrees with the two analytical-type methods quite well. The GRT results only include multiple reflections in the anomalous layer, which might cause the incomplete results of GRT. (C) displays the 2D and 3D synthetics along profile AA' in Figure 4A. 3D synthetics are generated by DWKM method (Helmberger and Ni, 2005), which approximates 3D wave propagation by summing the contribution from the Lit and the Diffraction zones. Here we only considered two Lit zones. The top diagram displays the ray paths sampling the structure with the magenta dash lines. In the bottom row, 3D synthetics are the summations of the left Lit and right Lit contributions.

Figure S6. 2D synthetics for moving the low velocity structure AA' in Figure 4E to source side.

Figure S7. (A) Data (black) and PREM synthetics (red) for three events along the

azimuth to the dense network (TriNet) in Southern California. They waveforms appear to be PREM-like as in Figure 2A. (B) The SP_dKS entering points (black crosses) at the CMB for all three events. The pink shading area indicates the sampling region with PREM-like records. This area includes the dense dataset from stations at Southern California. The blue dash lines outline the size of the Fresnel zone (FZ) with assuming the source period of 8 secs. The FZ is bigger than the lateral dimension of sampling region. If there's significant structure in the source region, we will predict some disturb waveforms for all azimuths. For the receiver side, the sampling region is much larger than the FZ as in Fig. S1B. If the same size anomaly structure is presented at receiver side, it will only affect profile along particular azimuth. Thus, it appears that the source region is PREM-like.

Figure S8. The measured SKKS-SKS differential travel time related to IASP model for the three events. The different colors relate to the azimuths for particular records.

Figure S9. Stacked records along two distinct azimuths (green: 29-37° and red: 43-60°) for the three events. The records are aligned on the SKS arrivals.

Figure S10. The same stacked records as in Figure S10 but aligned on the SKKS arrivals. Note that the SKS_d phase tracks the timing of SKKS very well.

Reference

Helmberger, D. V., Ni, S., 2005. Approximate 3D body-wave synthetics for tomographic models. *Bull. Seismol. Soc. Am.* 95, 212-224.

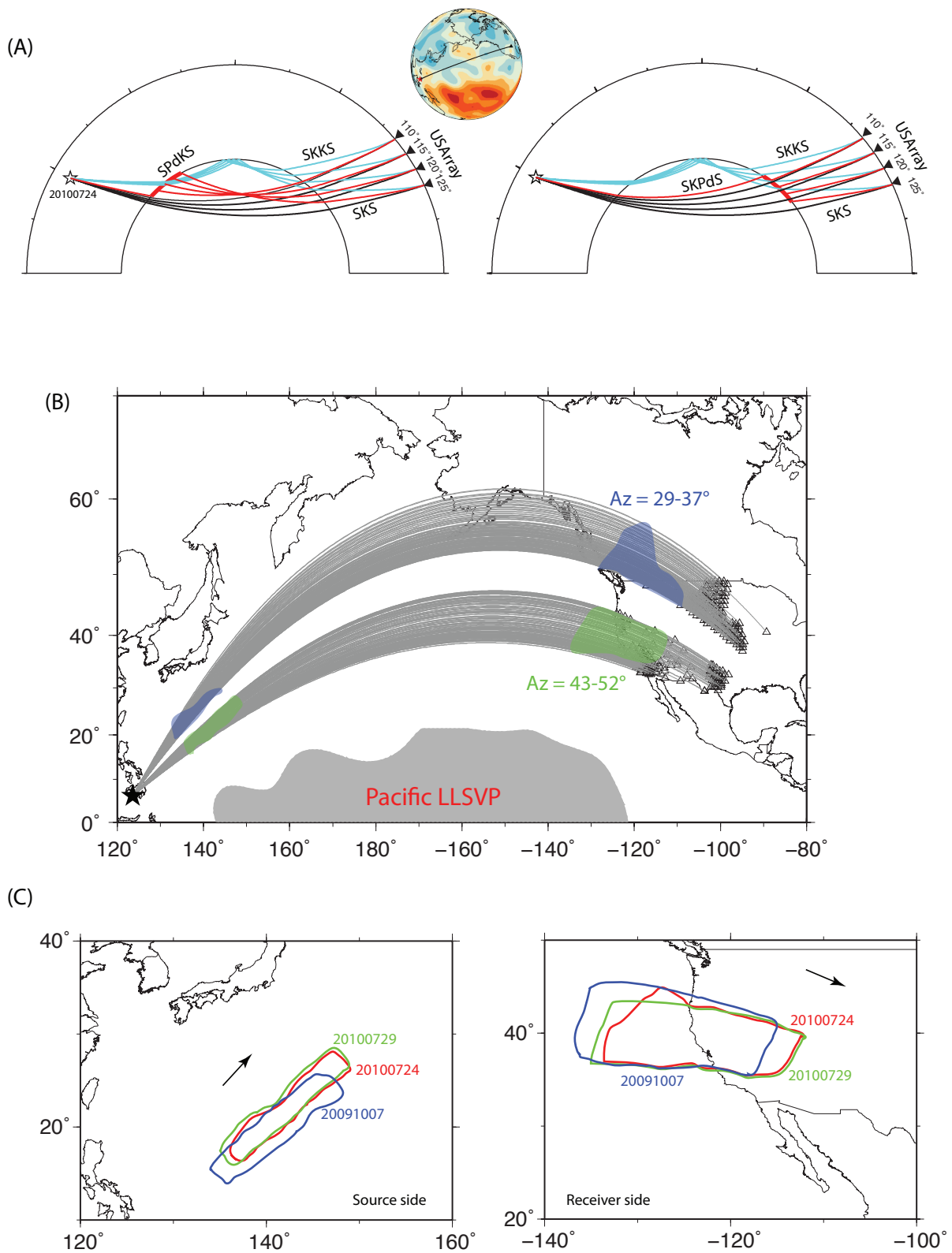


Figure S1

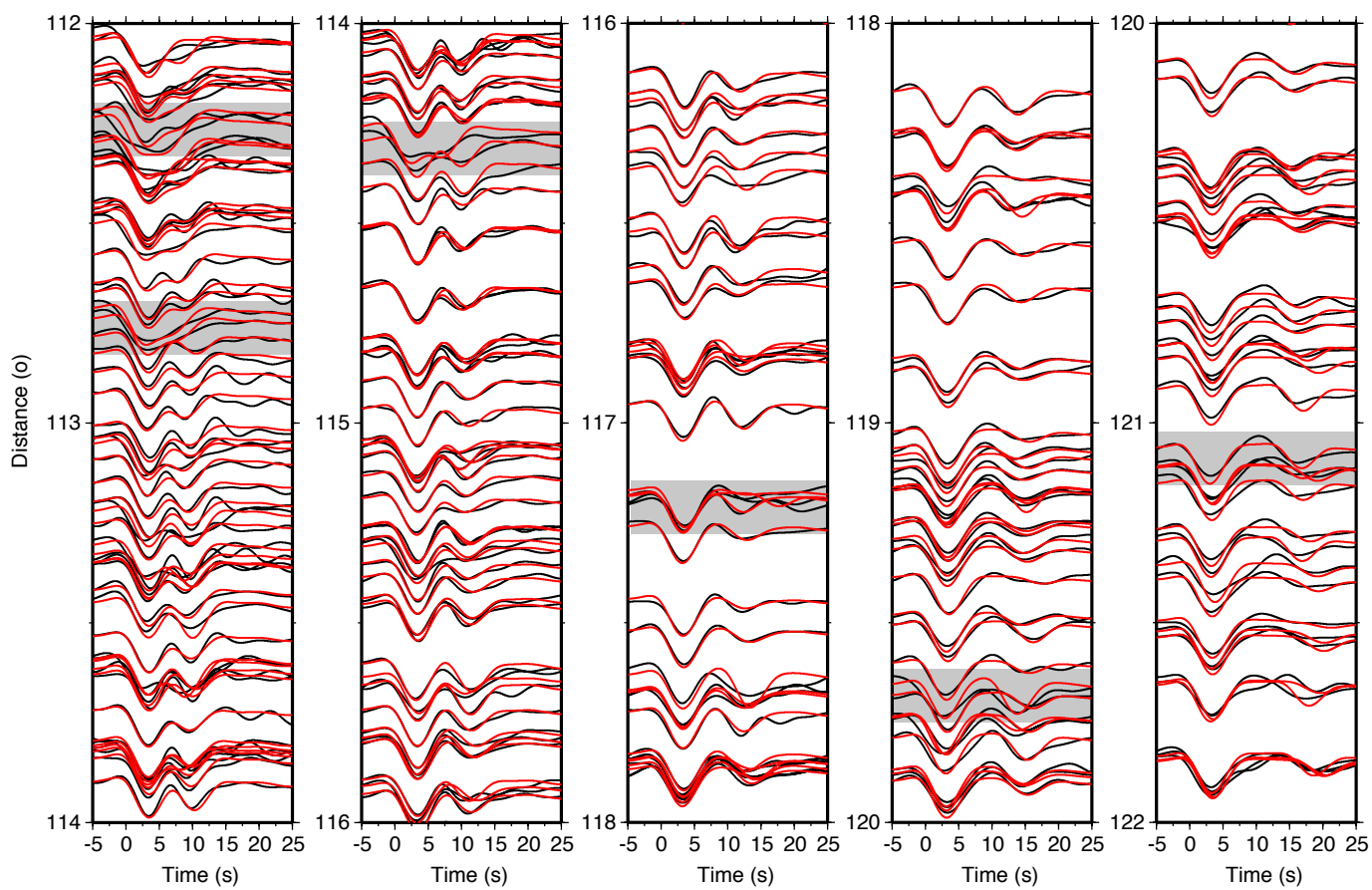


Figure S2

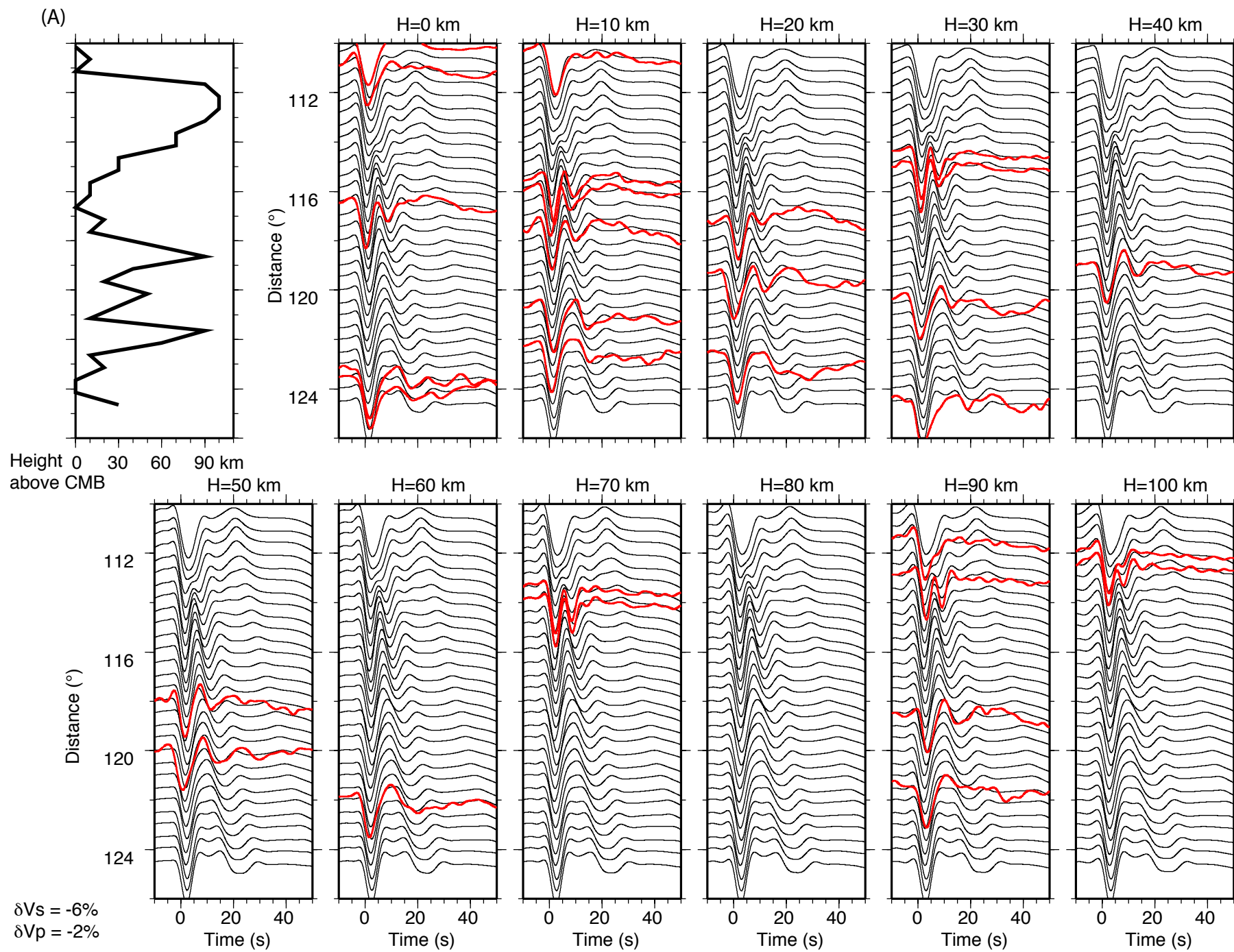


Figure S3

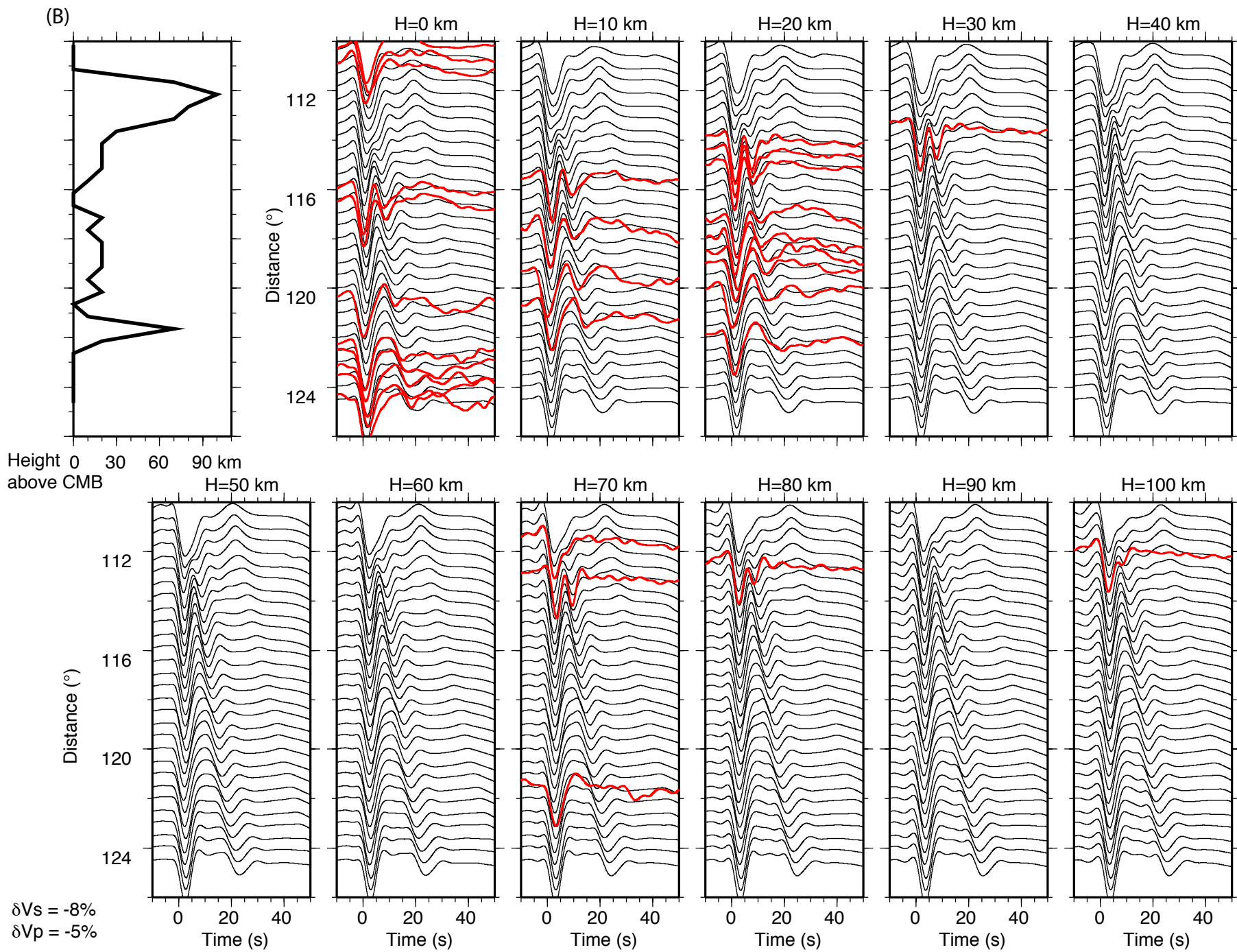


Figure S3

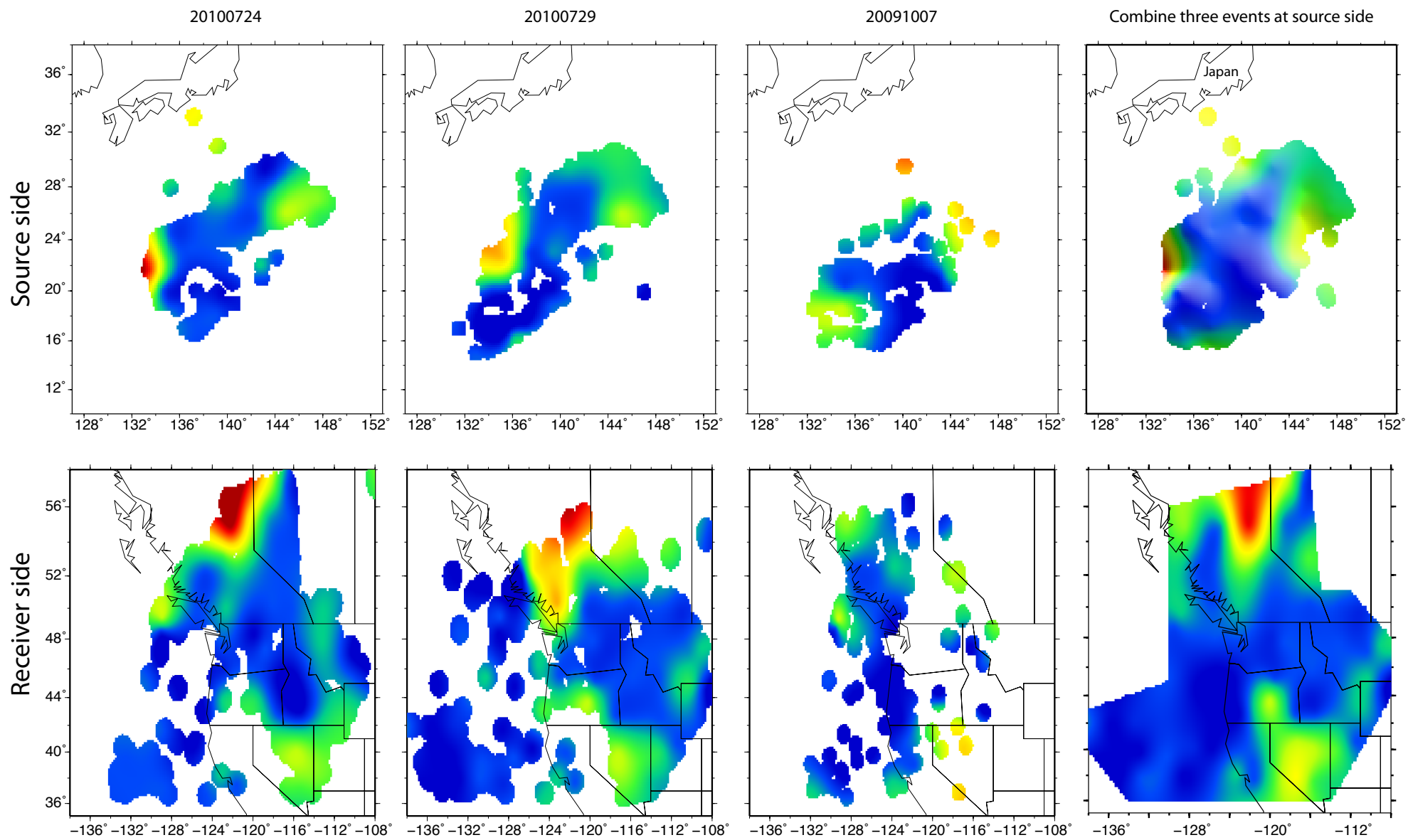


Figure S4

(A)

Uniform layer: $H = 60\text{km}$, $dV_s = -10\%$, $dV_p = -5\%$

FD

f-k

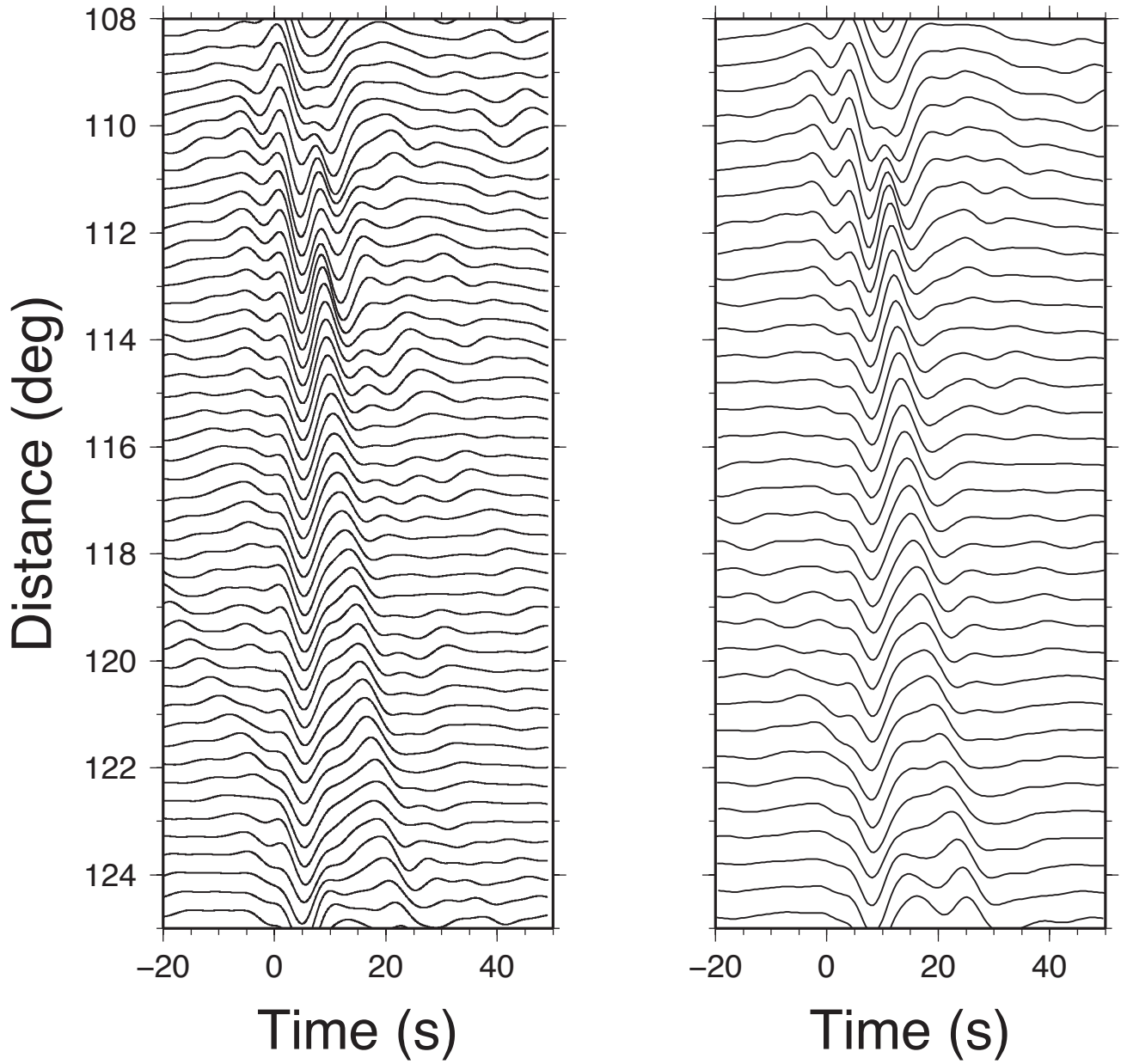


Figure S5

(B)

Source side layer: $H = 60\text{km}$, $dV_s = -10\%$, $dV_p = -5\%$

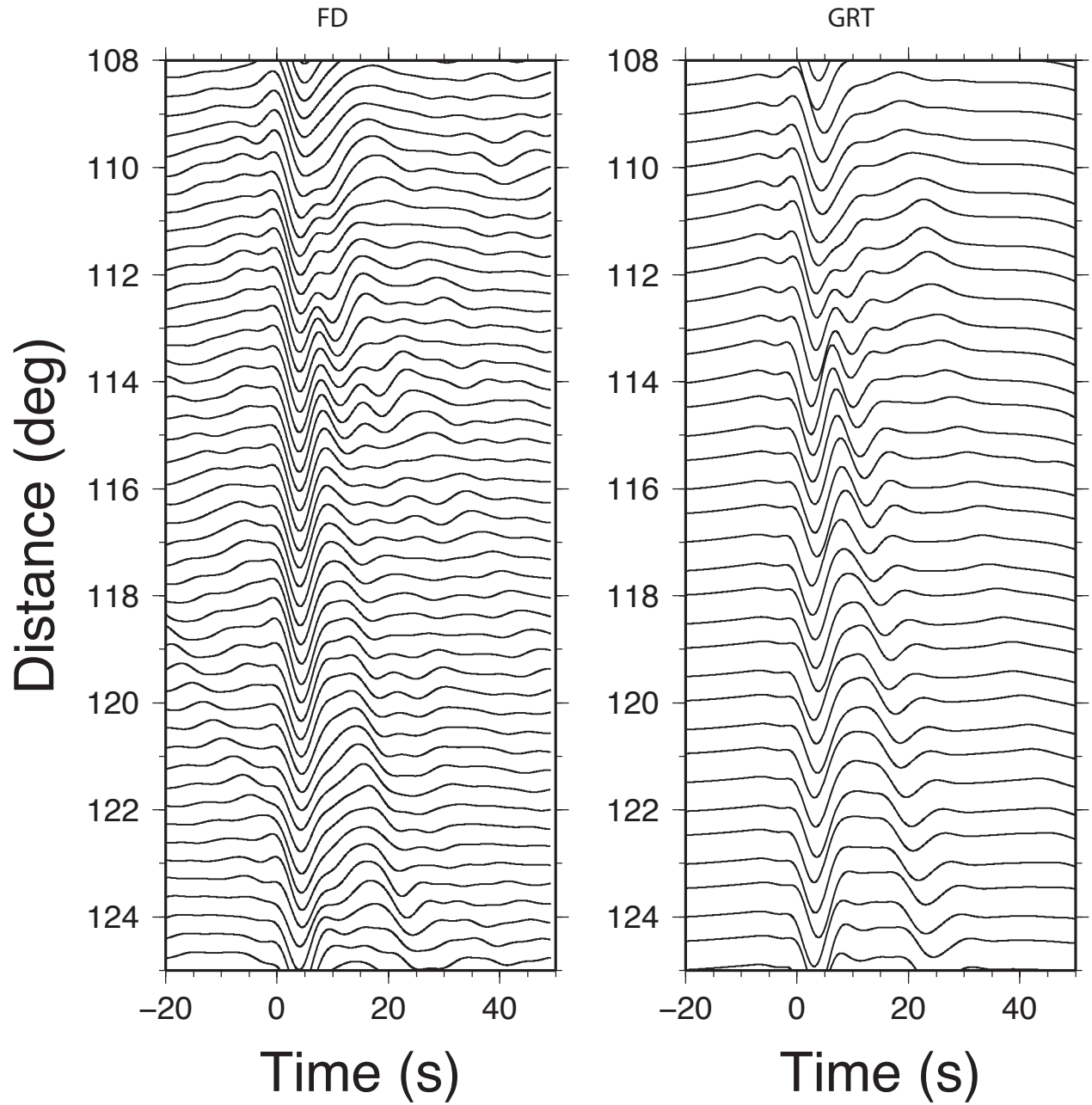


Figure S5

(C)

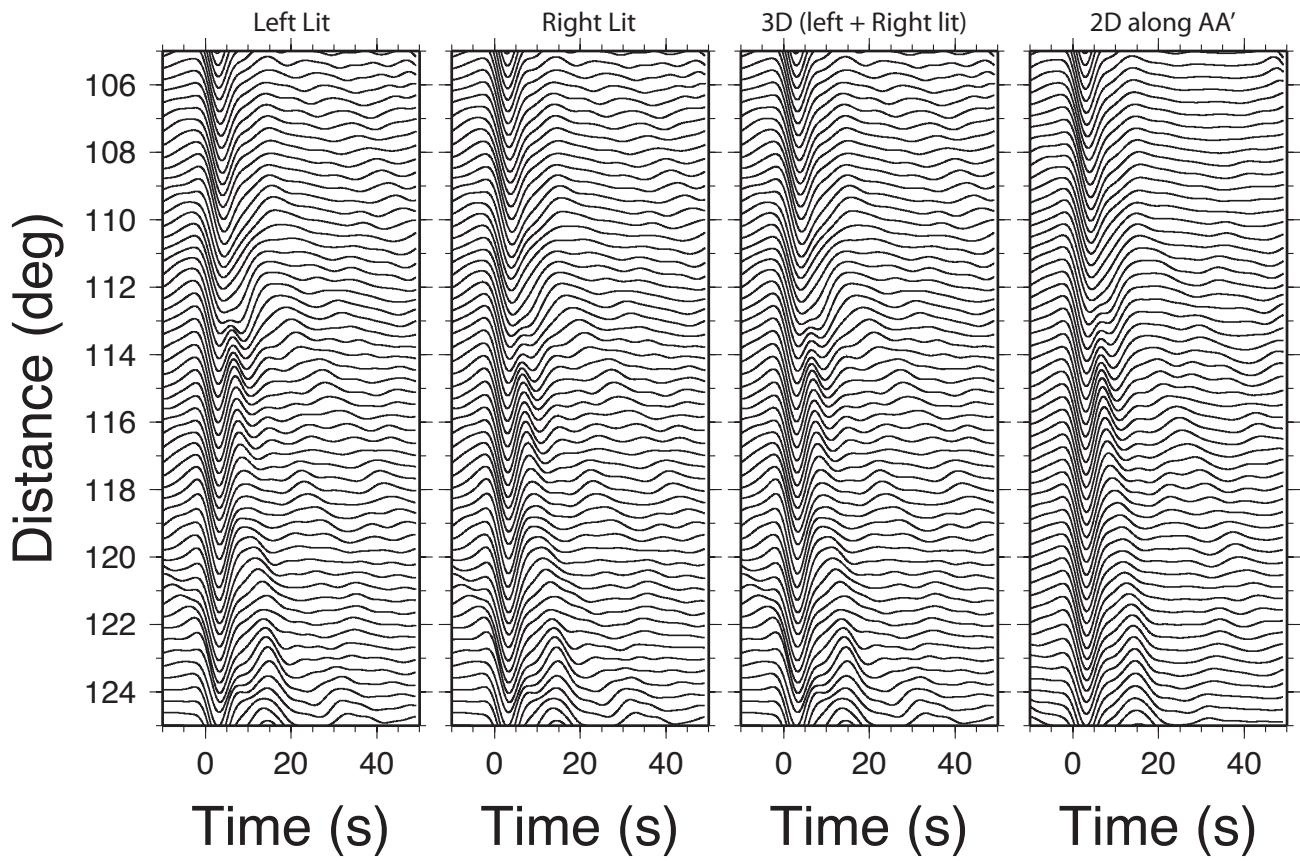
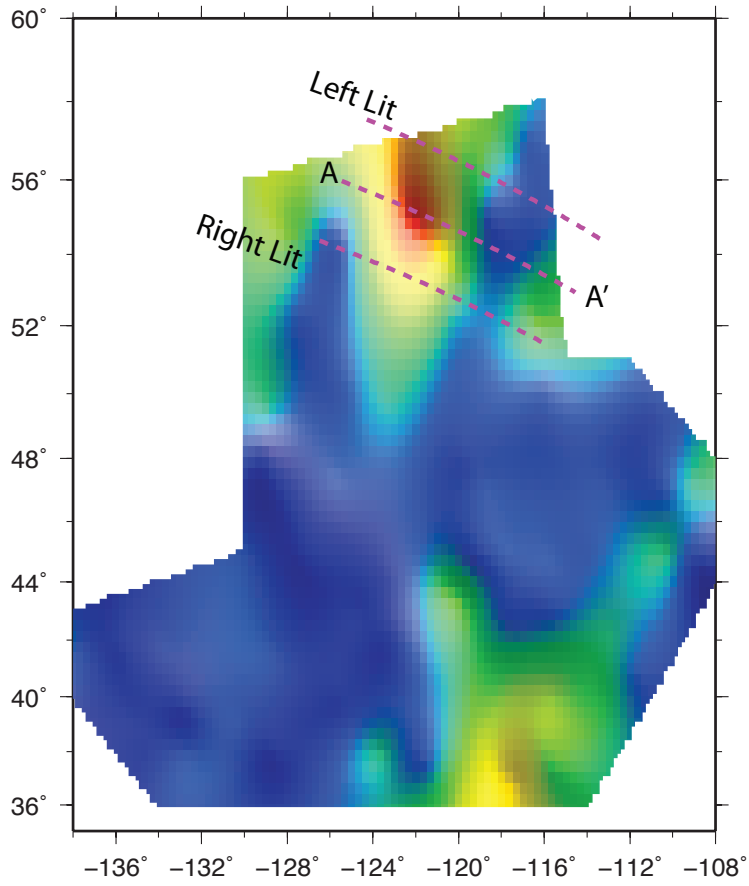


Figure S5

Black: stacked data along AA' as in Fig. 4E
Red: synthetics for structure along AA' at source side

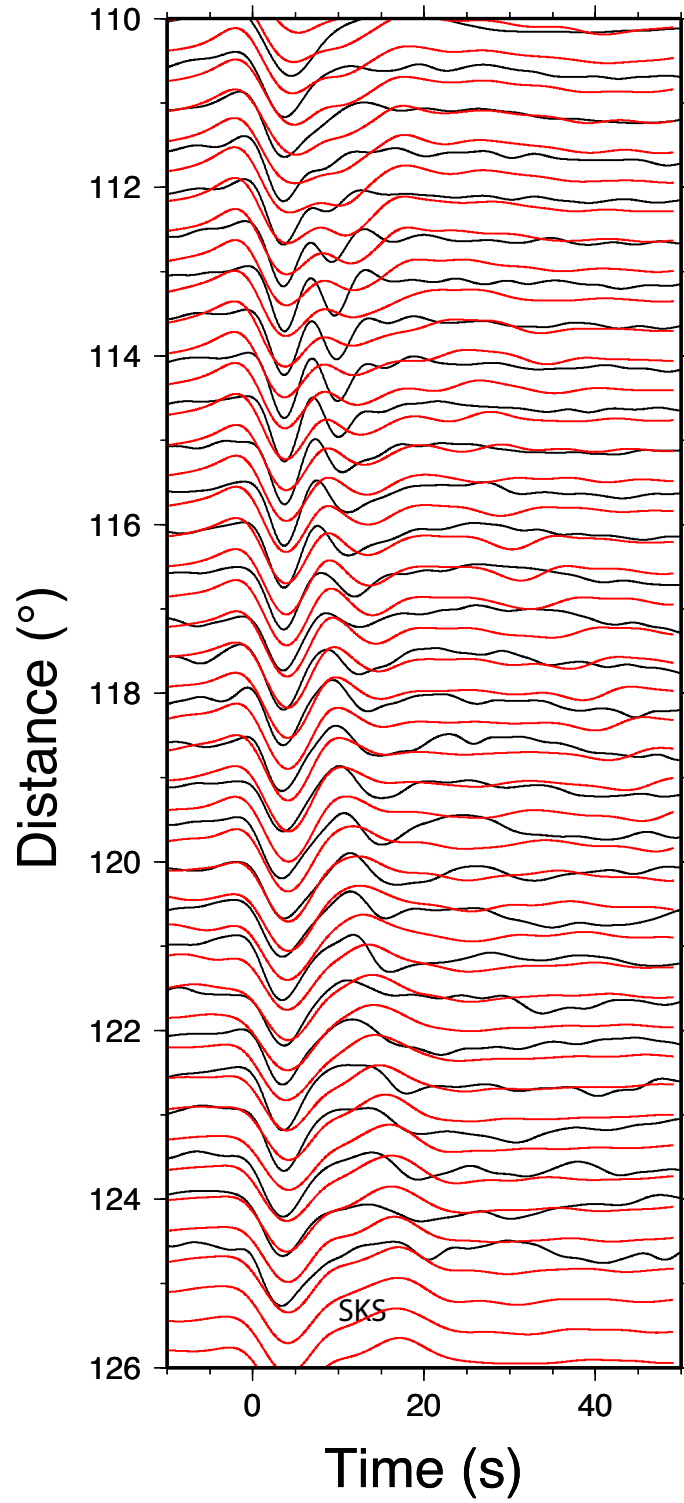


Figure S6

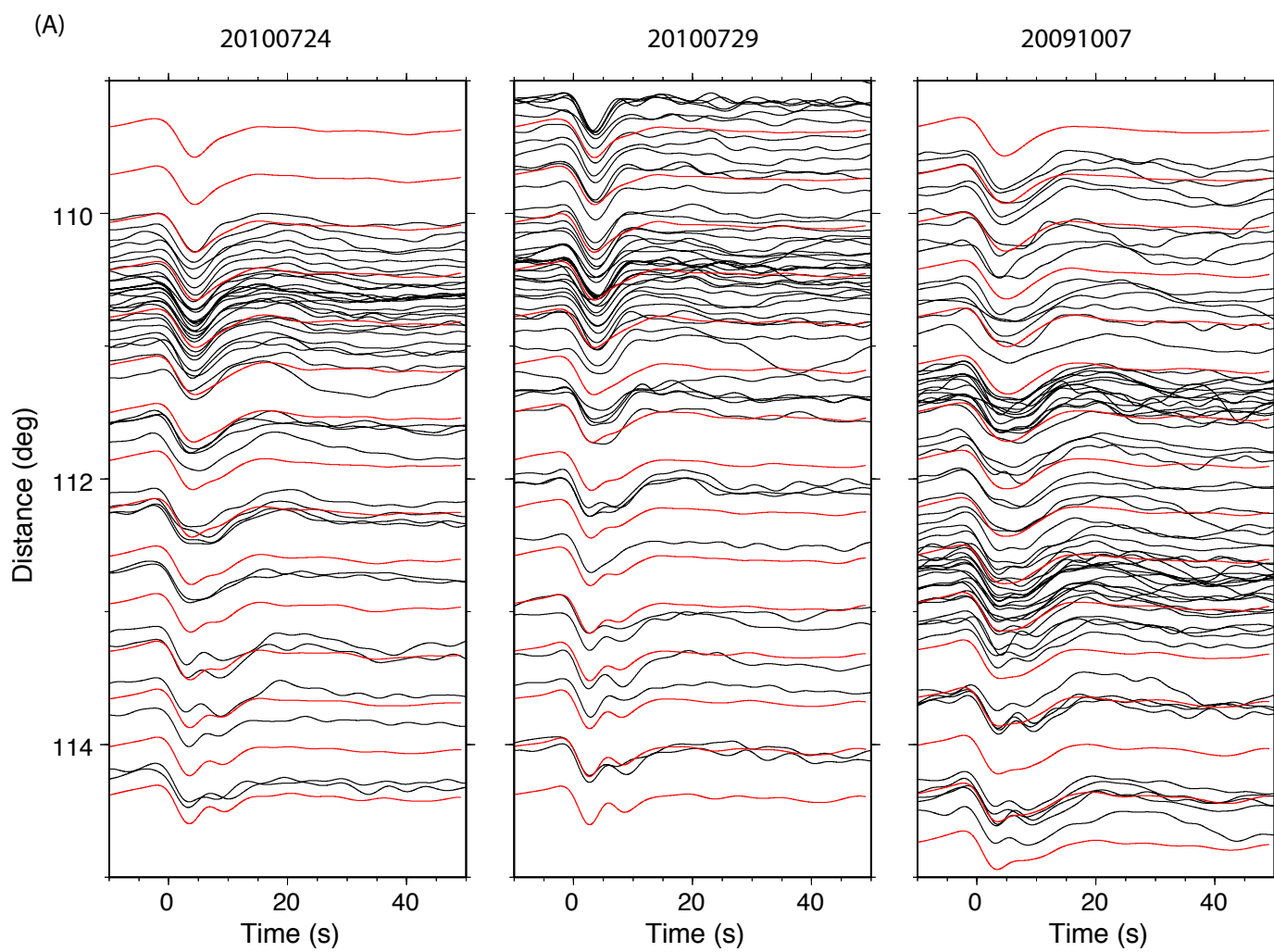


Figure S7

(B)

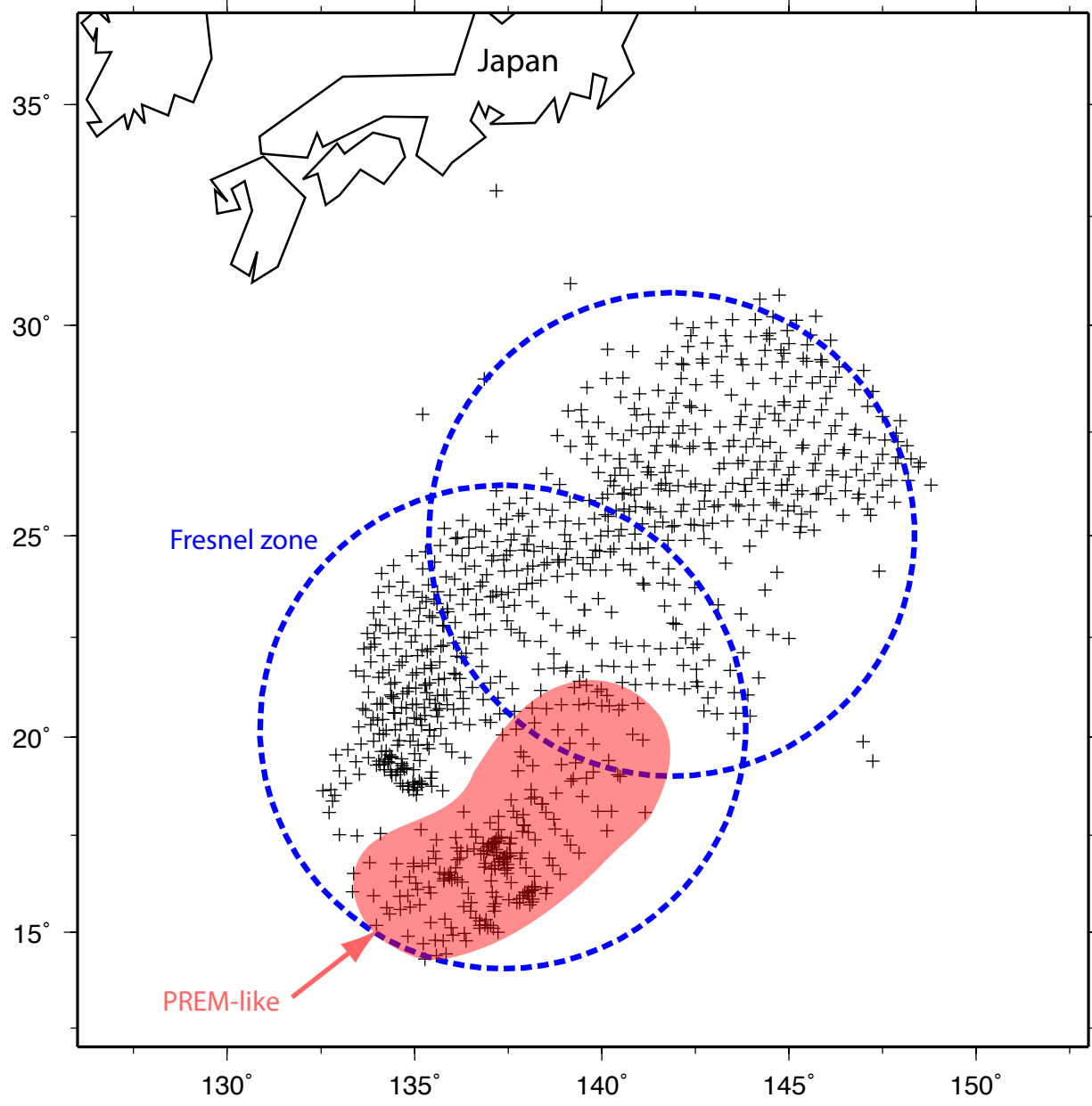


Figure S7

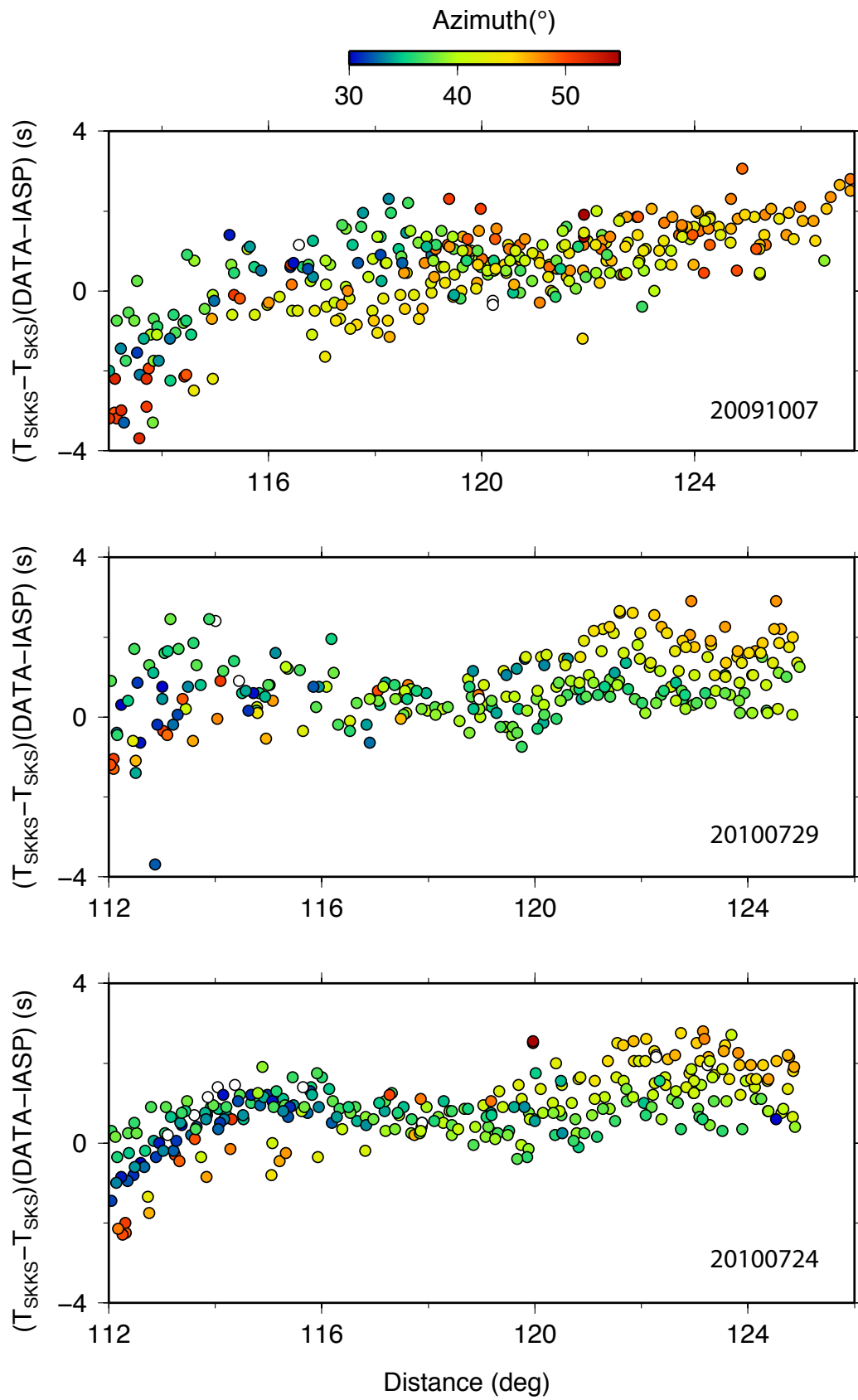
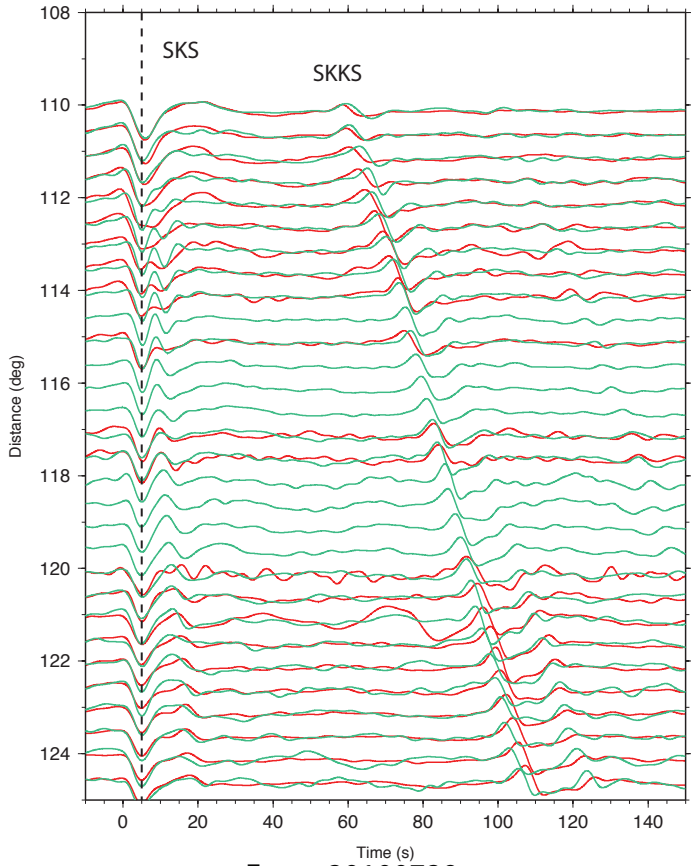


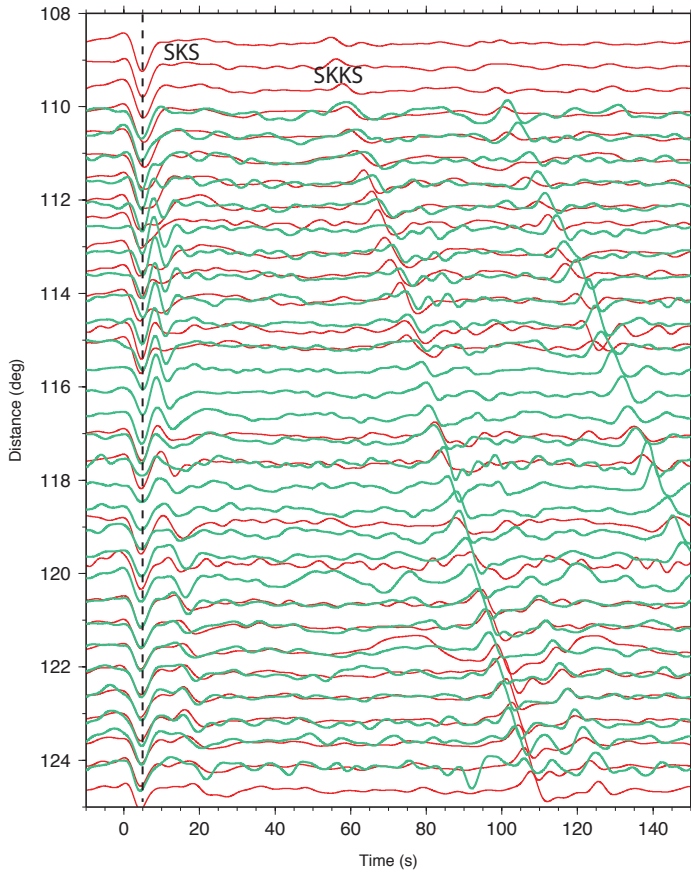
Figure S8

Event 20100724



Azimuth 29~37°
Azimuth 43~60°

Event 20100729



Event 20091007

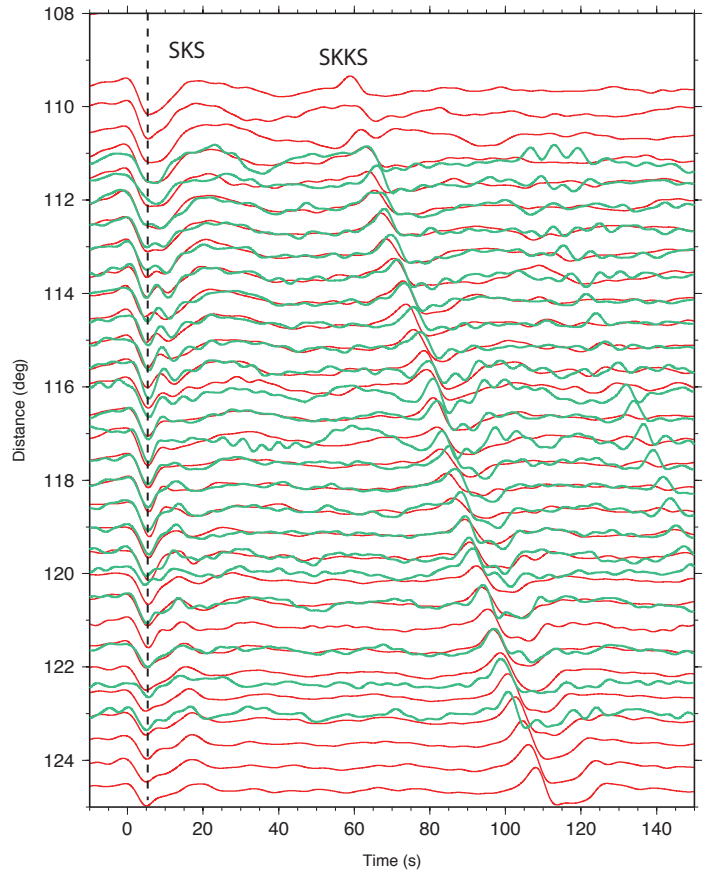
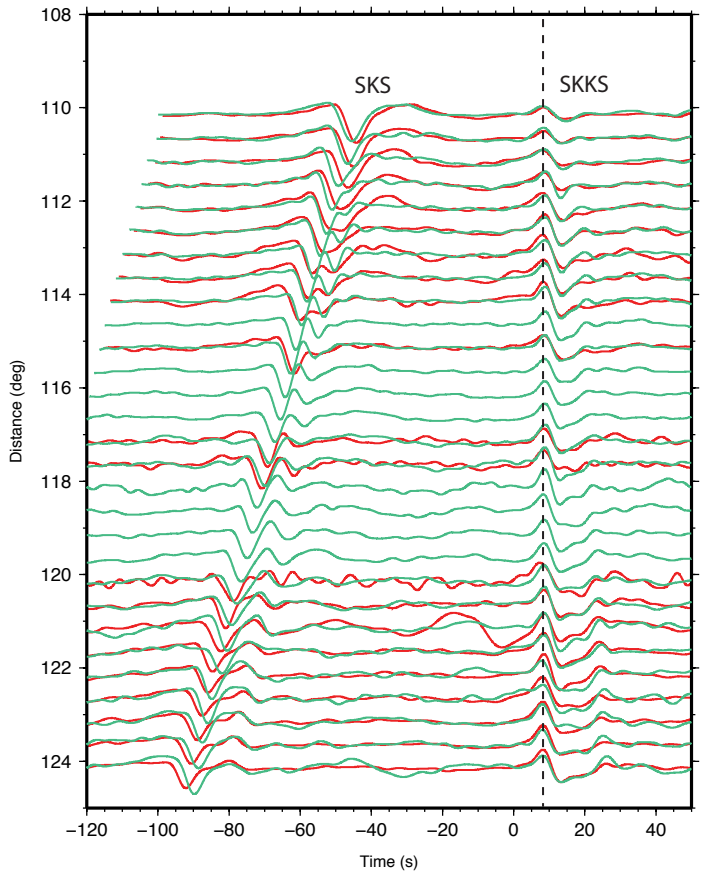


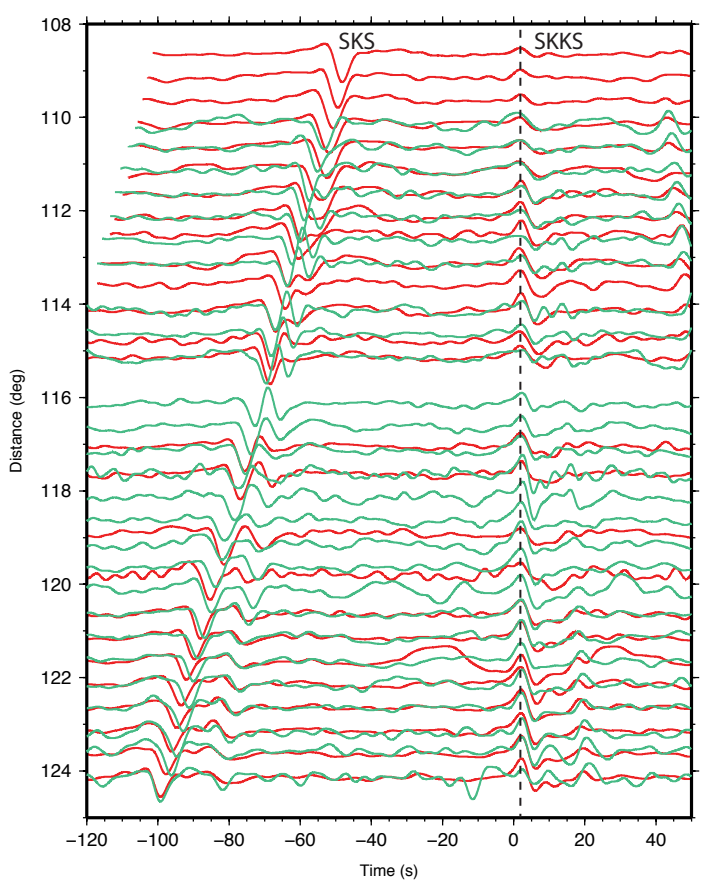
Figure S9

Event 20100724



Azimuth 29~37°
Azimuth 43~60°

Event 20100729



Event 20091007

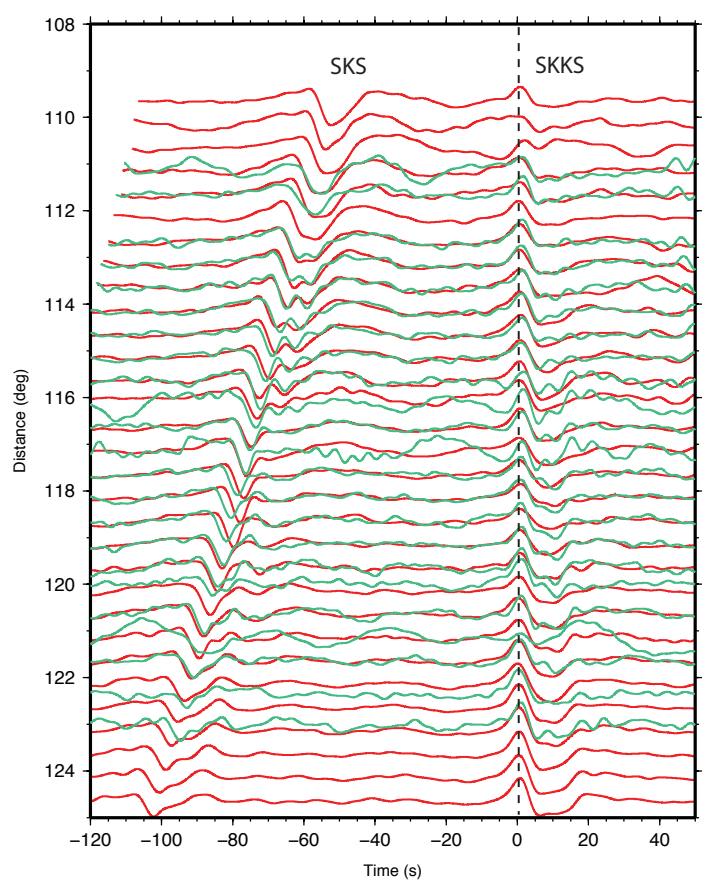


Figure S10